Journal of Catalysis 268 (2009) 150–155

Contents lists available at ScienceDirect

Journal of Catalysis

journal homepage: www.elsevier.com/locate/jcat

Kinetics and particle size effects in ethene hydrogenation over supported palladium catalysts at atmospheric pressure

Axel Binder [a,*], Martin Seipenbusch [a], Martin Muhler [b], Gerhard Kasper [a]

[a] Institut für Mechanische Verfahrenstechnik und Mechanik, Karlsruher Institut für Technologie (KIT), Straße am Forum 8, D-76131 Karlsruhe, Germany
[b] Technische Chemie, Ruhr-Universität Bochum, Universitätsstr. 150, D-44801 Bochum, Germany

ARTICLE INFO

Article history:
Received 9 July 2009
Revised 15 September 2009
Accepted 15 September 2009
Available online 13 October 2009

Keywords:
Ethene hydrogenation
Particle size effect
Structure sensitivity
Supported palladium catalyst
Chemical vapor deposition (CVD)
Chemical vapor synthesis (CVS)

ABSTRACT

Palladium catalysts were synthesized in a highly controlled chemical vapor deposition process, giving narrowly distributed Pd nanoparticles with median sizes ranging from 1.3 to 5 nm on a SiO_2 or TiO_2 support. Unsupported Pd nanoparticles with median sizes between 3 and 9 nm were also generated by spark discharge.

The influence of Pd particle size and support on the hydrogenation of ethene to ethane was investigated in a fixed-bed flow reactor at atmospheric pressure. The TOF was found to peak at 3 to 4 nm with a weak dependence on the support material. Metal support interactions were generally weak, indicated by closely matching activation energies of 20 kJ mol^{-1} for unsupported Pd, and 28 kJ mol^{-1} for titania and silica supported catalysts. Peak TOF values varied systematically with H_2 partial pressure, indicating a pronounced volume effect of the Pd particles on the reactivity.

1. Introduction

Palladium catalysts are predominantly used in hydrogenation and dehydrogenation reactions of hydrocarbons. A large number of these reactions are known to be structure sensitive [1], a phenomenon which has been intensively investigated for supported metal catalysts [2,3]. The hydrogenation of ethene is extensively studied and a general reaction mechanism was proposed by Horiuti and Polanyi [4], in which ethene is hydrogenated by dissociated hydrogen atoms being sequentially added to the adsorbed alkene intermediates. In the literature, the structural sensitivity of the hydrogenation of ethene is under debate and is believed to be nonexistent by some authors [2]. Kinetic studies of Schlatter and Boduard for instance indicated that the rate at which ethene hydrogenates is independent of the particle size [5]. Additionally, Shaikhutdinov and Rupprechter reported that the activity of ethene hydrogenation is independent of the particle size over $Pd/Al_2O_3/NiAl(1\,1\,0)$ between 1 and 6 nm, respectively [6,7]. In contrast to these studies Borodziński reported a slight increase of the turnover frequency (TOF) of the hydrogenation of ethyne in ethyne–ethene mixtures on a Pd/SiO_2 catalyst in the particle size range of 1–30 nm [8]. Other studies showed that the TOF in the hydrogenation of ethyne in ethyne–ethene mixtures on Pd/Al_2O_3 catalysts rises with increasing particle size [9–11]. In addition to the experimental findings, Monte-Carlo simulations demonstrated a strong increase of turnover frequency (TOF) for the ethene hydrogenation on Pd/SiO_2 catalysts in size range of 0–40 nm [12].

A possible reason for these apparent discrepancies in the literature may be found in the variation of experimental conditions and materials. Most experimental studies were conducted on ideal systems such as metal foils and ideal conditions such as high vacuum and in excess H_2. The transfer of these results to real process conditions is therefore questionable. Furthermore, to our knowledge experimental data for Pd supported on different materials at comparable conditions are unavailable, hindering the assessment of catalyst support interactions.

In the present work, we report the hydrogenation of ethene on nanoscale catalyst particles at atmospheric conditions with special emphasis on the influence of the Pd particle size on the reactivity to understand structure-function relationships of this reaction at industrially relevant process conditions. We studied the reactivity of unique narrowly distributed Pd particles on inert supports such as silica, on active supports such as titania and unsupported Pd particles to exclude metal–support interactions as an obstruction in the determination of structural sensitivity.

* Corresponding author. Fax: +49 721 6086563.
E-mail addresses: axel.binder@kit.edu (A. Binder), martin.seipenbusch@kit.edu (M. Seipenbusch), muhler@techem.ruhr-uni-bochum.de (M. Muhler), gerhard.kasper@kit.edu (G. Kasper).

0021-9517/$ - see front matter © 2009 Elsevier Inc. All rights reserved.
doi:10.1016/j.jcat.2009.09.013

2. Experimental

2.1. Catalyst preparation

Supported palladium catalyst particles were generated in the gas phase by a combined chemical vapor synthesis (CVS) and metal–organic chemical vapor deposition (MOCVD) process, which was described in detail in previous publications [13,14]. Ultrafine silica and titania support particles were generated by thermal decomposition of their metal alkoxide vapors in a CVS process [15]. For this, the alkoxide tetraethylorthosilicate ($Si(OC_2H_5)_4$, TEOS) and titanium tetraisopropoxide ($Ti(OC_3H_7)_4$, TTIP) were evaporated at 50 and 75 °C, respectively, and then fed to a tube furnace, where the vapors were mixed with oxygen and a diluting nitrogen flow. The precursors oxidize into highly super-saturated oxide phases and particle formation takes place by homogeneous nucleation. This first step of particle formation is followed by condensation of the growth species on the newly formed particles and subsequent surface reactions. Agglomeration of the highly concentrated aerosol particles results in fractal structures with surface areas up to 350 $m^2 g^{-1}$. Downstream, the aerosol was sintered at 1500 °C to obtain spherical particles with well-defined surfaces. The resulting mean particle sizes were about 80 nm with geometric standard deviations of 1.3. The particle number concentration was 10^7 cm^{-3} at a total flow rate of 300 ml min^{-1}.

The support particles were coated with palladium directly in the aerosol state via MOCVD using the metal–organic compound cyclopentadienyl-allyl-Pd [Cp(allyl)Pd; synthesized by the working group of Prof. Fischer, Lehrstuhl für Anorganische Chemie II, Ruhr Universität Bochum]. The palladium precursor concentration was 1.4×10^{-7} mol l^{-1} at a temperature of 80 °C in the CVD reactor.

The unsupported palladium particles were synthesized using a spark discharge generator [16], consisting of two palladium-electrodes in parallel with a capacitor charged by a high-voltage source and nitrogen (1 l min^{-1}, 99.99%) as carrier gas. The charging of the capacitor leads to an increase in the potential difference between the electrodes until the breakthrough voltage is reached. The energy stored in the capacitor is then released into a spark plasma, which provides the energy for the evaporation of the material from the electrode surfaces but also creates a large quantity of ions which are accelerated in the decaying electric field, and physically removed the material from the electrodes by sputtering. The particle generation subsequently occurs by condensation of the metal atoms in the cold carrier gas. The particle size depends mainly on the material and lies in the range between 2 and 6 nm.

2.2. Catalytic activity and kinetic measurements

For the catalytic experiments the catalyst particles were collected on a polycarbonate membrane filter (diameter 45 mm, pore size 0.2 μm) which was placed downstream of the coating reactor. To obtain large palladium particle sizes the catalyst particles were sintered prior to deposition in the aerosol state in a tube furnace (residence times of about 30 s) downstream of the coating reactor and were then collected on a filter.

The set-up of the catalytic experiments is shown in Fig. 1. For each experiment all tubing, the filter and the IR chamber, which is a self-made chamber with a length of 224 mm, were flushed with nitrogen and hydrogen. A flow of ethene (1 ml min^{-1}, 99.9%), hydrogen (1 ml min^{-1}, 99.9%), and dilution nitrogen (50 ml min^{-1}, 99.99%) bypassing the reactor was directed to an FTIR (Bruker Vector 22), where the ethene concentration was detected between wave numbers of 500 and 4000 cm^{-1} with a resolution of 4 cm^{-1}. The rates were detected by the decrease in the ethene concentration when directing the flow through the filter (Fig. 1, right). For determination of the ethene concentration, the spectra between wave numbers of 1810 and 1960 cm^{-1} were integrated. This peak was chosen for analysis because there is no overlaying of the spectra of ethene and ethane (Fig. 1, inset right). Please note that this band is not easy to be related to a specific band but should be allocated to the harmonic of the CH_2-wagging.

The palladium particle sizes were determined by transmission electron microscopy (TEM) image analysis before and after reaction. The TEM images were recorded on a Philips CM 12 electron microscope operating at 120 kV. The particle size distributions were expressed in terms of log-normal distributions. The total palladium mass of each catalytic sample was determined by inductively coupled plasma optical emission spectrometry (ICP-OES).

Additional information about the shape of the Pd particles would be helpful but an alternative determination of the Pd particle size by H_2 or CO chemisorption was not possible because the total Pd mass of every sample was simply too low. Furthermore, additional complications would arise, such as hydrogen spill-over on Pd/TiO_2, and the multiple bondings of CO as a function of the Pd particle size, which would end in misleading results. Thus, we preferred to derive the TOF based on the well-established TEM image analysis of the Pd particle sizes with sufficiently narrow particle size distributions.

All catalytic experiments were performed at atmospheric pressure at a constant temperature of 293 K. The turnover frequencies were expressed in mol ethane per second and per mol palladium

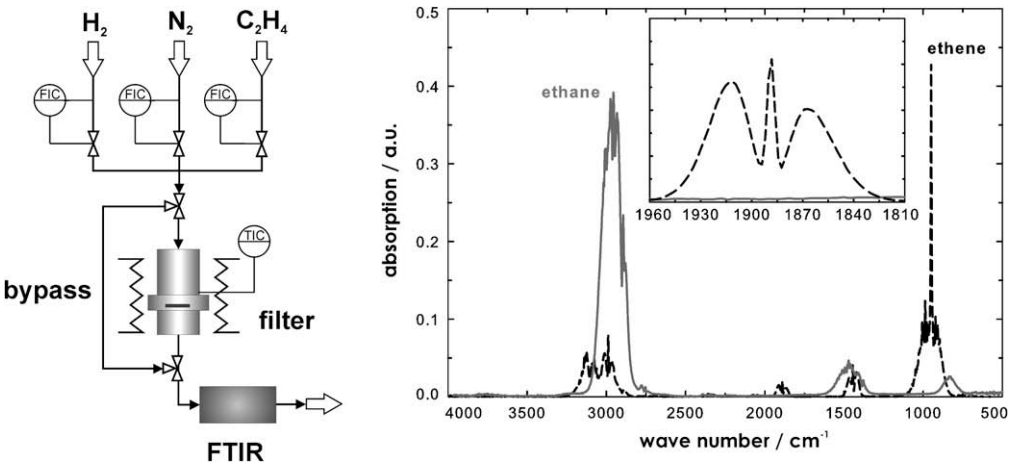

Fig. 1. Experimental set-up of the catalytic experiments (left) and IR spectra of ethene and ethane (right) and spectra range for conversion measurements (inset).

surface atoms. The palladium surfaces were calculated by the total palladium mass determined by ICP-OES and the mean palladium diameter determined by TEM image analyses assuming semi-spherical palladium particles on the surface of the support particles.

The ethene concentration dependence was measured at a reaction temperature of 293 K and a hydrogen concentration of 3.4×10^{-9} mol l^{-1} (partial pressure 76.9 mbar) for palladium on a silica support. The ethene concentration was varied from 1.4×10^{-9} to 5.5×10^{-9} mol l^{-1} (partial pressures 30.8–123 mbar).

The hydrogen concentration dependence was also measured at a reaction temperature of 293 K and an ethene concentration of 4.1×10^{-9} mol l^{-1} (partial pressure 90.9 mbar). The hydrogen concentration was varied from 8.1×10^{-10} to 2.0×10^{-8} mol l^{-1} (partial pressures 18.2–455 mbar).

The temperature dependence was measured for palladium supported on silica and titania and for unsupported palladium particles generated by spark discharge. The reaction was carried out in a temperature range between 283 and 313 K. The ethene and hydrogen concentrations were 7.3×10^{-10} mol l^{-1} (partial pressures of 16.4 mbar).

To study the influence of the palladium particle size on the TOF of ethene hydrogenation several samples with different palladium particle sizes were prepared by variation of the MOCVD conditions and/or by sintering of the deposited palladium particles. We prepared palladium particles supported on silica and titania in a size range of 1.8–4.4 and 1.3–5.1 nm, respectively. The reaction was carried out at 293 K and atmospheric pressure. The ethene and hydrogen concentrations were set to 7.3×10^{-10} mol l^{-1} (partial pressures of 16.4 mbar). We compared these results to unsupported palladium in size range of 3.1–8.7 nm.

3. Results and discussion

3.1. Morphology of catalyst particles

The morphology of the supported Pd particles is shown in Fig. 2. The deposited Pd particles from the MOCVD process were distributed log-normally with mean diameters in the range of 1.3–3 nm, depending on Pd precursor concentration, and very small geometric standard deviations of about 1.1 (for more detailed information see [13]). Also the deposited and sintered Pd particles could be described by log-normal distributions with small geometric standard deviations of about 1.2. The unsupported Pd particles generated by spark discharge were also distributed very narrowly so the samples could be characterized in terms of mean diameters. Because of the very narrowly distributed Pd particle sizes and their precise determination this process supplies ideal model catalyst particles.

The purity of the oxide carrier particles as well as the obtained Pd coatings was analyzed by energy-dispersive X-ray (EDX) analysis up to 10 keV. High-purity particles and coatings were found which contain no detectable carbon contamination (compare [13]). Electron diffractions obtained by TEM indicates that the Pd particles have a crystalline structure, while the support particles are more or less amorphous.

3.2. Kinetics of ethene hydrogenation at atmospheric conditions

Fig. 3 shows the plot of ln (TOF) versus ln (ethene pressure) for Pd particles with a mean diameter of 4.2 nm supported on silica, where the ethene partial pressure is expressed in mbar. A fit to the data yields the reaction order in ethene pressure of 0.39 ± 0.01. This value differs from reaction orders in ethene

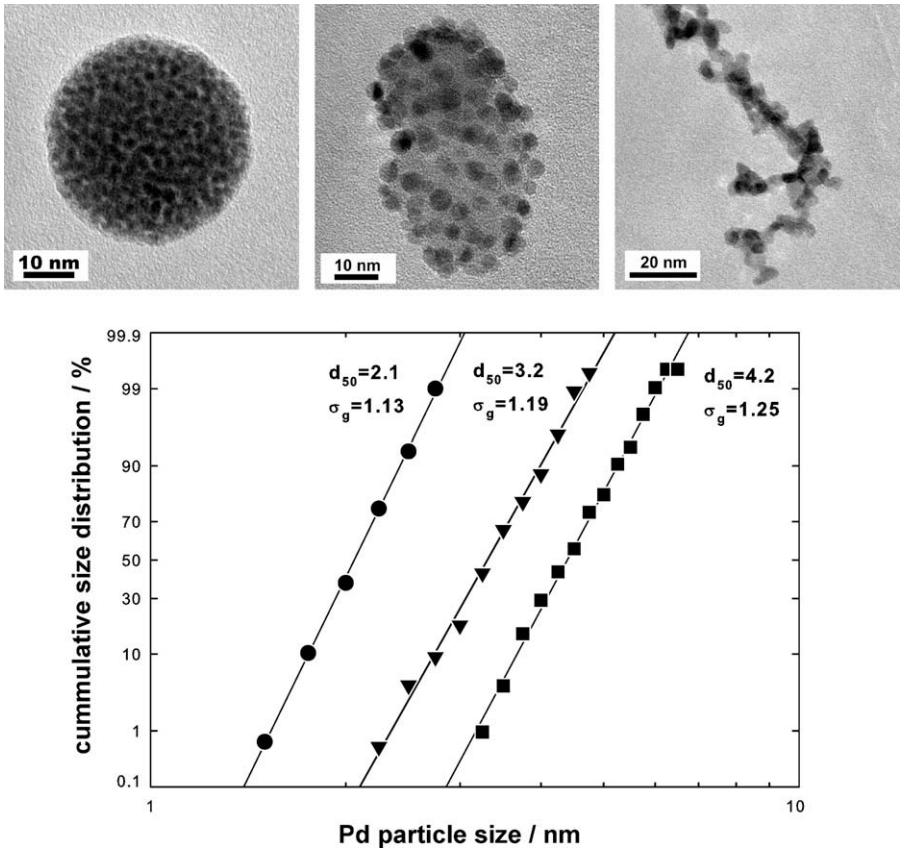

Fig. 2. Top row: TEM images of silica-supported Pd after the coating reactor (left, ●), sintered at 873 K (middle, ▼), and unsupported Pd catalyst particles sintered at 473 K (right, ■). Below: corresponding cumulative distributions of the projected Pd diameters.

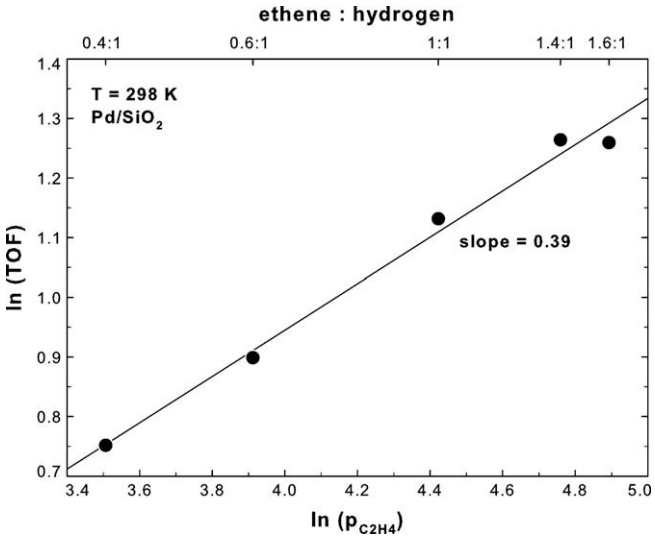

Fig. 3. Plot of ln (TOF) versus ln (ethene partial pressure). Reaction temperature was 298 K at atmospheric pressure and H_2 concentration was set to 3.4×10^{-9} mol l^{-1}.

reported in the literature which were described to be nearly zero, for example a value of −0.03 on silica-supported palladium at 243 K [17] and negative like −0.22 for Pd(1 1 1) at 320 K [18]. A better agreement was found with orders for Pt/SiO_2 catalysts of 0.25 at 233 K [17]. Precise comparisons are difficult because this value clearly depends on reaction conditions such as temperature and pressure as Hansen and Neurock found in their Monte-Carlo simulation of the hydrogenation of ethene on a Pd(1 0 0) surface. They reported reaction orders in ethene between −0.4 and 0 or slightly positive at 298 K depending on ethene pressure [19].

The hydrogen pressure dependence was also determined for Pd particles with a mean diameter of 4.2 nm supported on silica. The resulting plot of ln (TOF) versus ln (hydrogen pressure), where the hydrogen partial pressure is expressed in mbar, is shown in Fig. 4. The reaction order determined from the slope of the best fit to the data was 1.04 ± 0.07.

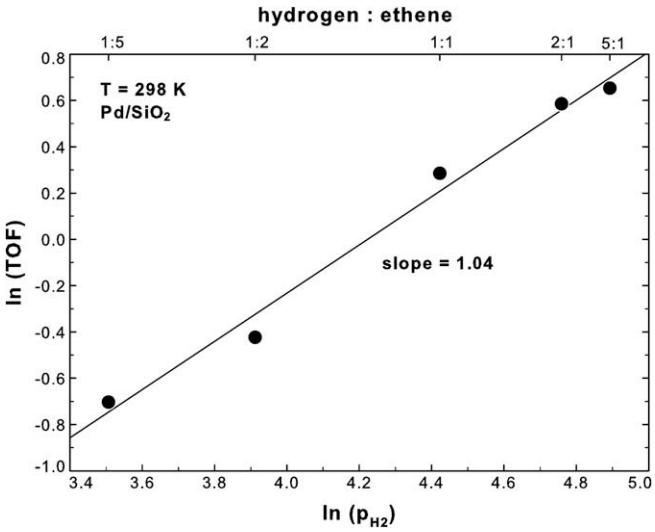

Fig. 4. Plot of ln (TOF) versus ln (hydrogen partial pressure). Reaction was performed at 298 K at atmospheric pressure and C_2H_4 concentration of 8.1×10^{-10} mol l^{-1}.

For silica-supported Pd a value of 0.66 was reported in the literature for a reaction temperature of 243 K [17], which can be explained by the temperature dependence of the reaction order [20]. Additionally, a value of 1 was found for alumina-supported Pd [21,22] and of 1.03 on a Pd(1 1 1) surface at 300 K [18].

The variation of the reaction temperature was studied for Pd supported on SiO_2 and TiO_2, and for unsupported Pd particles. Fig. 5 shows the results of the temperature dependence plotted as ln (rate constant) versus inverse temperature. The activation energies calculated from the slopes are given in Table 1.

Reported activation energies for ethene hydrogenation of supported Pd and Pt catalysts vary between 25 and 46 kJ mol^{-1} [5,17] and are in good agreement with our values which are on the lower end of the scale. The value of the unsupported Pd is also in the range of reported activation energies for Pd and Pt single crystals between 12.6 kJ mol^{-1} on the Pd(1 1 1) surface [23] and 45 kJ mol^{-1} [18,24–26]. Only the values from Monte-Carlo simulations are slightly higher with 37–50 kJ mol^{-1} on the Pd(1 0 0) surface [19].

To conclude, ethene hydrogenation at the investigated conditions is in good agreement with the reported data in the literature with the exception of the reaction order in ethene, which seems slightly too high. The activation energies show virtually identical values for Pd on different supports. A slightly lower value for unsupported Pd indicates a small influence of the support.

3.3. Influence of palladium particle size on the reaction rate

The variation of the Pd particle size was investigated for Pd supported on silica and titania as well as on unsupported Pd particles. The resulting TOFs as a function of Pd particle diameter are plotted in Fig. 6.

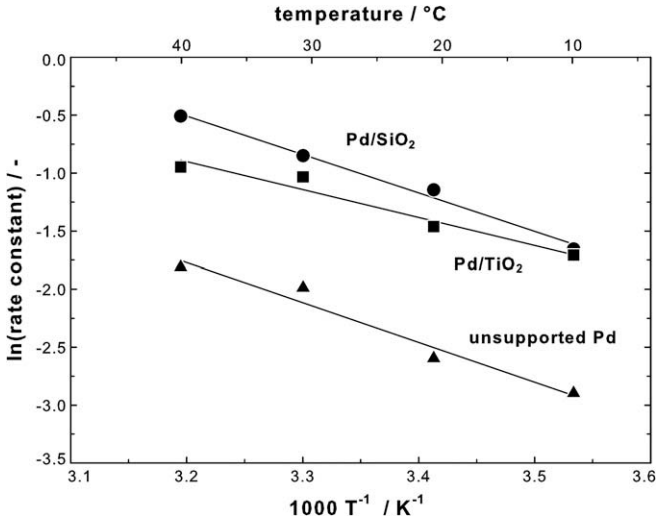

Fig. 5. Arrhenius plot for ethene hydrogenation catalyzed by Pd/SiO_2 (●), Pd/TiO_2 (■), and unsupported Pd (▲). Reactions were conducted at atmospheric pressure with H_2 and C_2H_4 concentrations of 7.3×10^{-10} mol l^{-1}.

Table 1
Activation energies for the hydrogenation of ethene on Pd/SiO_2, Pd/TiO_2, and unsupported Pd at atmospheric pressure with hydrogen and ethene concentrations of 7.3×10^{-10} mol l^{-1} and temperature range of 283–313 K.

Sample	Calculated activation energy (kJ mol^{-1})	Palladium particle size (nm)
Pd/SiO_2	27.6 ± 0.27	4.2
Pd/TiO_2	26.9 ± 1.06	4.2
Unsupported Pd	20.0 ± 0.93	5.1

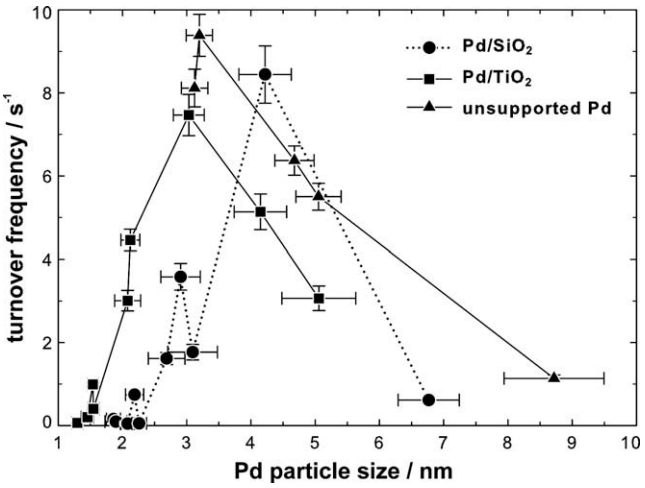

Fig. 6. TOF versus Pd particle size for Pd/SiO_2 (●), Pd/TiO_2 (■), and unsupported Pd (▲) and for the hydrogenation of ethene. Reaction was carried out at atmospheric pressure at a reaction temperature of 293 K; H_2 and C_2H_4 concentrations were 8.6×10^{-4} mol l^{-1}.

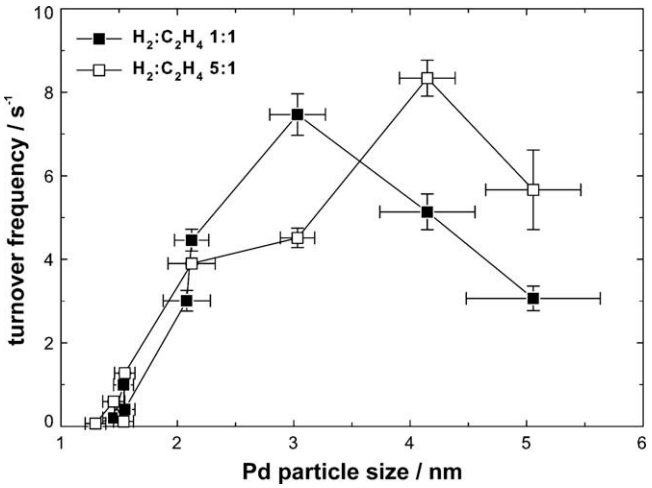

Fig. 7. TOF versus Pd particle size for Pd/TiO_2 (■, H_2:C_2H_4 = 1:1 and □, H_2:C_2H_4 = 5:1, left) for the hydrogenation of ethene. Reaction was carried out at atmospheric pressure at reaction temperature of 293 K and ethene concentration of 8.6×10^{-4} mol l^{-1}.

The plot demonstrates a clear dependence of the TOF on Pd particle size. For the titania-supported Pd and the unsupported Pd a maximum TOF is observed at a particle size of 3 nm, while for silica supported Pd the maximum of the rate seems to be at larger particle sizes of about 4 nm. This shift in the size with maximum activity is maybe caused by the influence of the support material and indicated a small metal–support interaction between Pd and silica at these conditions. The activity for all catalysts is about 8-fold higher for the maximum rates in comparison to the lowest values. One can also see that the support has no strong influence on the maximum activity with measured values of TOF being very similar for unsupported Pd (9.4 s^{-1}), Pd/SiO_2 (8.4 s^{-1}), and Pd/TiO_2 (7.5 s^{-1}). Similar results were reported by Arakawa for the hydroformylation of ethene measuring the ethane by-production over a Rh/SiO_2 catalyst finding a maximum of TOF for a particle size of 4 nm [27].

It is commonly believed that the π-bonded ethene hydrogenates to ethane [21,28,29]. Additionally, the activation of molecular π-bonds requires a unique configuration of several metal atoms or step-edge sites, respectively, in which the π-bond dissociates through multiple contacts with several surface atoms [30]. Such step sites can physically not be present below a particular particle size. The relative probability of such sites is a function of particle size and shows a maximum which could be an explanation for the maximum of the TOF [31].

Another possible explanation for the observed size effect is based on Doyle's demonstration of the importance of the subsurface H_2 as the active species in the hydrogenation reaction. The authors investigated the hydrogenation of ethene on both Pd(1 1 1) single crystals and Pd particles supported on an Al_2O_3/NiAl(1 1 0) film under low-pressure conditions [32,33]. They reported that on Pd(1 1 1) no hydrogenation occurs while palladium particles were highly active at the same conditions. The authors concluded that in the nanoparticle dimensions the subsurface hydrogen is accessible to the adsorbed alkene while for the Pd(1 1 1) surface the hydrogen atoms diffuse deeply into the bulk and are thus not readily available for the reaction at the surface. The decrease in the TOF for larger particles could thus also be a result of a volume effect, where the increasing particle volume decreases the accessibility of the subsurface hydrogen. For small particles on the other hand volume can also provide an explanation for decreasing activity below the optimum particle size. If subsurface hydrogen is indeed crucial for the reaction the storage capability of the particles is an important factor which will be correlated to the particle volume. In that case other stoichiometric compositions, i.e. an excess of H_2 should influence the TOF or the maximum activity, respectively. Higher H_2 concentrations should not influence the activity of the small Pd particles because of their limited storage capacity but increase the activity of the larger ones due to an increase in availability of subsurface hydrogen. Consistently, the reaction order in H_2 should be size dependent and it was indeed shown that it is decreasing with increasing particle size [34]. Fig. 7 shows the resulting TOF on Pd/TiO_2 as a function of the Pd particle size for an excess of H_2 (H_2:C_2H_4 = 5:1, unfilled symbols). Indeed, one can see that the maximum activity for Pd/TiO_2 shifts from a Pd particle size of 3 nm for stoichiometric conditions to larger particles sizes of about 4.2 nm for excess H_2.

This influence of H_2 partial pressure on the optimal Pd particle size could also be the reason for the contradictory results reported by Shaikhutdinov ([Pd/Al_2O_3/NiAl(1 1 0)], H_2:C_2H_4 = 3:1, −183 °C, vacuum) and Masson (Pt on amorphous Al_2O_3 film, H_2:C_2H_4 = 10:1, 100 °C, 1 atm) who found an independence of TOF in the Pd particle size range of 1–3 nm and 1.7–2.8 nm, respectively [6,35]. These results are contradictory to the structure sensitivity reported here, but both studies cover very small Pd particle size ranges, which are in particular lower than the observed maximum of the TOF at excess H_2 in this study (see Fig. 7).

4. Conclusion

The hydrogenation of ethene over narrowly distributed supported palladium nanoparticle catalysts at atmospheric pressure was investigated. The rate for the hydrogenation of ethene catalyzed by palladium shows a clear size dependence in the size range of 1–9 nm for Pd supported on SiO_2 or TiO_2 and for unsupported Pd with peaks at 3–4 nm. The supports have nearly no influence on the structure sensitivity behavior, indicating a negligible influence of the support for vapor deposited metal particles. This was supported by similar activation energies for the unsupported Pd particles (20 kJ mol^{-1}) and for Pd on silica and titania (27–28 kJ mol^{-1}). The results clarify a strong volume effect of the Pd where the accessibility of the subsurface H_2 seems to be important. The influence of the H_2 concentration on the optimal Pd particle size for the reaction confirms this assumption.

The results underline the influence of process conditions on the structural sensitivity and thus emphasize on the importance of

compliance with realistic parameters in terms of educt concentrations in experimental investigations of industrial relevance.

Acknowledgments

This project was partially funded by Deutsche Forschungsgemeinschaft (DFG) in SPP 1119. The authors would also like to thank Prof. Fischer and co-workers (Lehrstuhl für Anorganische Chemie II, Ruhr Universität Bochum) for synthesizing the precursor and advising in matters of precursor chemistry.

References

[1] C.O. Bennett, M. Che, J. Catal. 120 (1989) 293–302.
[2] M. Che, C.O. Bennett, Adv. Catal. 36 (1989) 55–172.
[3] G.C. Bond, Surf. Sci. 156 (1985) 966–981.
[4] I. Horiuti, M. Polanyi, Trans. Faraday Soc. 30 (1934) 1164–1172.
[5] J.C. Schlatter, M. Boudart, J. Catal. 24 (1972) 482–492.
[6] S. Shaikhutdinov, M. Heemeier, M. Baumer, T. Lear, D. Lennon, R.J. Oldman, S.D. Jackson, H.J. Freund, J. Catal. 200 (2001) 330–339.
[7] G. Rupprechter, Ann. Rep. Prog. Chem. Sect. C 100 (2004) 237–311.
[8] A. Borodzinski, Catal. Lett. 71 (2001) 169–175.
[9] C.E. Gigola, H.R. Aduriz, P. Bodnariuk, Appl. Catal. 27 (1986) 133–144.
[10] H.R. Adúriz, P. Bodnariuk, M. Dennehy, C.E. Gigola, Appl. Catal. 58 (1990) 227–239.
[11] S. Hub, L. Hilaire, R. Touroude, Appl. Catal. 36 (1988) 307–322.
[12] A.S. McLeod, Chem. Eng. Res. Des. 82 (2004) 945–951.
[13] A. Heel, G. Kasper, Aerosol Sci. Technol. 39 (2005) 1027–1037.
[14] A. Binder, A. Heel, G. Kasper, Chem. Vap. Depos. 13 (2007) 48–54.
[15] K. Okuyama, Y. Kousaka, N. Tohge, S. Yamamoto, J.J. Wu, R.C. Flagan, J.H. Seinfeld, AlChE J. 32 (1986) 2010–2019.
[16] S. Schwyn, E. Garwin, A. Schmidt-Ott, J. Aerosol Sci. 19 (1988) 639–642.
[17] G.C.A. Schuit, L.L. Vanreijen, Adv. Catal. 10 (1958) 242–317.
[18] H. Molero, D. Stacchiola, W.T. Tysoe, Catal. Lett. 101 (2005) 145–149.
[19] E.W. Hansen, M. Neurock, J. Catal. 196 (2000) 241–252.
[20] H. Molero, B.F. Bartlett, W.T. Tysoe, J. Catal. 181 (1999) 49–56.
[21] T.P. Beebe, J.T. Yates, J. Am. Chem. Soc. 108 (1986) 663–671.
[22] A.N.R. Bos, E.S. Bootsma, F. Foeth, H.W.J. Sleyster, K.R. Westerterp, Chem. Eng. Process. 32 (1993) 53–63.
[23] D. Stacchiola, S. Azad, L. Burkholder, W.T. Tysoe, J. Phys. Chem. B 105 (2001) 11233–11239.
[24] F. Zaera, G.A. Somorjai, J. Am. Chem. Soc. 106 (1984) 2288–2293.
[25] R.D. Cortright, S.A. Goddard, J.E. Rekoske, J.A. Dumesic, J. Catal. 127 (1991) 342–353.
[26] J.E. Rekoske, R.D. Cortright, S.A. Goddard, S.B. Sharma, J.A. Dumesic, J. Phys. Chem. 96 (1992) 1880–1888.
[27] H. Arakawa, N. Takahashi, T. Hanaoka, K. Takeuchi, T. Matsuzaki, Y. Sugi, Chem. Lett. (1988) 1917–1918.
[28] P.S. Cremer, G.A. Somorjai, J. Chem. Soc.-Faraday Trans. 91 (1995) 3671–3677.
[29] H.J. Freund, M. Bäumer, J. Libuda, T. Risse, G. Rupprechter, S. Shaikhutdinov, J. Catal. 216 (2003) 223–235.
[30] R.A. van Santen, Acc. Chem. Res. 42 (2009) 57–66.
[31] R. van Hardeveld, A. van Montfoort, Surf. Sci. 4 (1966) 396–430.
[32] A.M. Doyle, S.K. Shaikhutdinov, S.D. Jackson, H.J. Freund, Angew. Chem. Int. Ed. 42 (2003) 5240–5243.
[33] A.M. Doyle, S.K. Shaikhutdinov, H.J. Freund, J. Catal. 223 (2004) 444–453.
[34] R.M. Rioux, R. Komor, H. Song, J.D. Hoefelmeyer, M. Grass, K. Niesz, P. Yang, G.A. Somorjai, J. Catal. 254 (2008) 1–11.
[35] A. Masson, B. Bellamy, Y.H. Romdhane, M. Che, H. Roulet, G. Dufour, Surf. Sci. 173 (1986) 479–497.